

Kinetic laws at the collapse transition of a homopolymer

Yu. A. Kuznetsov, E. G. Timoshenko, and K. A. Dawson

Theory Group, Centre for Soft Condensed Matter and Biomaterials, Department of Chemistry, University College Dublin, Dublin 4, Ireland

(Received 28 September 1995; accepted 28 November 1995)

We present results from numerical analysis of the equations derived in the Gaussian self-consistent method for kinetics at the collapse transition of a homopolymer in dilute solution. The kinetic laws are obtained with and without hydrodynamics for different quench depths and viscosities of the solvent. Some of our earlier analytical estimates are confirmed, and new ones generated. Thus the first kinetic stage for small quenches is described by a power law decrease in time of the squared radius of gyration with the universal exponent $\alpha_i=9/11$ (7/11) with (without) hydrodynamics. We find the scaling laws of the characteristic time of the coarsening stage, $\tau_m \sim N^{\gamma_m}$, and the final relaxation time, $\tau_f \sim N^{\gamma_f}$, as a function of the degree of polymerization N . These exponents are equal to $\gamma_m=3/2$, $\gamma_f=1$ in the regime of strong hydrodynamic interaction, and $\gamma_m=2$, $\gamma_f=5/3$ without hydrodynamics. We regard this paper as the completion of our work on the collapse kinetics of a bead and spring model of a homopolymer, but discuss the possibility of studying more complex systems. © 1996 American Institute of Physics. [S0021-9606(96)50709-X]

I. INTRODUCTION

Study of the kinetic laws of the coil-to-globule transition of a simple homopolymer in dilute solution is an important prerequisite to understanding the conformational transitions of complex biological systems, such as protein and DNA folding. Equilibrium aspects of the homopolymer problem have been extensively studied and essentially understood.¹⁻⁴ Meanwhile, the kinetic laws of the collapse transition are by no means elucidated, though advances have been made by computer methods using Monte Carlo,^{5,6} Langevin,⁷ and molecular dynamics⁸ simulations. It seems quite likely that these numerical studies have led to a correct qualitative picture of the collapse kinetics, including the notion of several different kinetic stages. These approaches, however, either were based on some assumptions concerning the dynamical mechanism, not completely obvious from the principles of statistical mechanics,⁵ or they have met with some technical problems originating from the numerical methods, that do not allow one to study the late stages of kinetics with a good statistical accuracy.^{6,7} We here emphasize that our work aims to resolve clearly the kinetics of collapse of a bead and spring model which we approximate for analytical work by the Edwards Hamiltonian.² As mentioned earlier, there are alternative models, and the degree of agreement between models is as yet unclear. We return to this point again in the conclusion to our study.

Early theoretical progress in understanding the kinetics phenomena in polymeric systems^{9,10} was helpful, but has been rather limited mainly due to the absence of systematic methods of nonequilibrium statistical mechanics that are easily applicable to the problem. The Gaussian self-consistent approach,¹¹ which resembles the time-dependent Hartree approximation, has the merit of being precisely defined, flexible, and of general applicability to many classes of problems. Application of this method to the collapse kinetics¹² yields a set of nonlinear first order differential equations in

time that determine the correlation functions of the Fourier modes of monomer positions. At first sight these equations appear to be very complicated and in the work cited above we were able to analyze and resolve only the linear approximation over the initial Flory coil state without account of hydrodynamics. Even so, such an analysis elucidated an important mechanism of the first kinetic stage akin to spinodal decomposition in the internal metrics of the chain,¹² and offered a different picture of the detailed mechanism of collapse than that due to earlier works in Refs. 9 and 10. Nevertheless, the full range of kinetic process was not studied in this method.

Thus several of the important questions about kinetics at the collapse transition still remain unanswered. Among them we consider the scaling laws of the collapse time as a function of the degree of polymerization, the quench depth, and viscosity of the solvent.

In the present paper we shall describe the results from comprehensive numerical study of the self-consistency equations¹² describing kinetics after the quench to the region of the phase diagram corresponding to the collapsed globule. Taken together with the earlier paper in Ref. 12 that relied only on analytical estimates this paper we view as the conclusion to our studies of the Gaussian ensemble approach to collapse kinetics of a homopolymer.

We begin by noting that the numerical analysis for this paper is a considerable computational task, even comparable to the Monte Carlo simulation of analogous system on a lattice. However, the Gaussian self-consistent approach possesses certain advantages to the latter approach and to the direct Langevin simulation. First, we consider only observables that are already averaged over the statistical ensemble, thus avoiding any artifacts of improper ensemble sampling. Second, it is free of the lattice artifacts, leading to a partial freezing of certain movements within a dense cluster. This circumstance is crucial at deep quenches, where the Monte Carlo method cannot yet be considered reliable,⁶ and finally,

account of the hydrodynamic interaction is quite straightforward and simple in the Gaussian self-consistent method. Thus in the present approach, one may hope to achieve a good control of precision and avoid systematic error in determination of the kinetic laws. Also, here we deal with a numerical solution of a finite set of differential equations and the behavior of the solution can be related to theoretical consideration.

Of course, the Gaussian self-consistent method possesses some disadvantages discussed in more detail in Sec. IV. However, we have found that these do not affect those kinetic laws that can be independently tested by the Monte Carlo method. We will argue therefore, that it is an important approach for the study of collapse and folding kinetics of all polymers and biopolymers.

II. SELF-CONSISTENCY EQUATIONS

We describe the polymer in very dilute solution by the Langevin equation for the Fourier coordinates of monomers \mathbf{x}_q , $q=0, \dots, N-1$, where N is the degree of polymerization (see the Appendix for more detail),

$$\dot{x}_q^\alpha(t) = \sum_{\alpha', q'} H_{qq'}^{\alpha\alpha'} [x(t)] \left(-\frac{\partial V}{\partial x_{q'}^{\alpha'}} + \eta_{q'}^{\alpha'}(t) \right), \quad (1)$$

where hydrodynamic effects are incorporated via $H_{qq'}^{\alpha\alpha'}$, the Oseen hydrodynamic interaction tensor,^{2,12} and the noise has the second order correlation function,

$$\langle \eta_q^\alpha(t) \eta_{q'}^{\alpha'}(t') \rangle = (H^{-1})_{qq'}^{\alpha\alpha'} 2k_B T \delta(t-t'). \quad (2)$$

The potential, V , is typically taken to include the spring term as well as the excluded-volume interaction written in terms of the virial expansion,

$$V = \frac{\kappa}{2} \sum_m (\mathbf{x}_m - \mathbf{x}_{m-1})^2 + \sum_{L=2}^{\infty} u_L \sum_{m_1 \dots m_L} \prod_{i=1}^{L-1} \delta(\mathbf{x}_{m_1} - \mathbf{x}_{m_{i+1}}), \quad (3)$$

where κ is the spring constant, u_L are the virial coefficients and $m_1 \neq m_2 \dots \neq m_L$.

Briefly then, the underlying idea of the Gaussian self-consistent method^{11,12} consists in replacing the exact nonlinear Langevin equation (1) and Eq. (2) by a linear stochastic ensemble,

$$\zeta_q(t) \dot{x}_q^\alpha(t) = -\Delta V_q(t) x_q^\alpha + \eta_q^\alpha(t), \quad (4)$$

$$\langle \eta_q^\alpha(t) \eta_{q'}^{\alpha'}(t') \rangle = \zeta_q 2k_B T \delta(t-t') \delta_{\alpha\alpha'} \delta_{-qq'}, \quad (5)$$

where the effective potential, $\Delta V_q(t)$, and the effective friction, $\zeta_q(t)$, can be found from the self-consistency equations for the equal-time correlation function,

$$\mathcal{F}_q(t) \equiv \frac{1}{3} \langle |\mathbf{x}_q(t)|^2 \rangle. \quad (6)$$

With space-isotropic initial conditions all spatial components yield equal contributions. One can show that $\mathcal{F}_q(t)$ satisfies the nonequilibrium equation of motion,¹²

$$\frac{\zeta_q(t)}{2} \mathcal{F}_q(t) = k_B T - \Delta V_q(t) \mathcal{F}_q(t). \quad (7)$$

There is also a nonlinear algebraic equation for the effective potential. In Refs. 11 and 12 this has been derived in two lowest orders of the virial expansion. We here generalized the equations to arbitrary order. Thus for a ring polymer, we obtain

$$\Delta V_q(t) = k_q - \sum_{L=2}^{\infty} \hat{u}_L \sum_{m_1 \dots m_L} \sum_{i,j=1}^{L-1} \frac{d_{m_1 m_{i+1}, m_1 m_{j+1}}^{(q)} \bar{\Delta}_{ij}^{(L-1)}}{(\det \Delta^{(L-1)})^{5/2}}, \quad (8)$$

where $\hat{u}_L = u_L / (2\pi)^{3(L-1)/2}$. In this formula $\Delta^{(L-1)}$ is a matrix of the size $L-1$ with the matrix elements

$$\Delta_{ij}^{(L-1)} = D_{m_1 m_{i+1}, m_1 m_{j+1}}, \quad (9)$$

and their cofactors are denoted by $\bar{\Delta}_{ij}^{(L-1)}$. The correlations $D_{nn'}, mm'$ of monomer spatial positions \mathbf{x}_n may be expressed as the Fourier transforms of quantities (6),

$$D_{nn', mm'} \equiv \frac{1}{3} \langle (\mathbf{x}_n - \mathbf{x}_{n'}) (\mathbf{x}_m - \mathbf{x}_{m'}) \rangle = \sum_q d_{nn', mm'}^{(q)} \mathcal{F}_q. \quad (10)$$

Here, we have used the following notations:

$$d_{nn', mm'}^{(q)} = -\frac{1}{2} (d_{nm}^{(q)} + d_{n'm'}^{(q)} - d_{nm'}^{(q)} - d_{n'm}^{(q)}), \quad (11)$$

with $d_{nm}^{(q)} = 2 - 2 \cos(2\pi q(n-m)/N)$. In this notation the spring term may be written as $k_q = \kappa N d_{01}^{(q)}$.

The friction, $\zeta_q(t)$, can be calculated in the so-called "preaveraging" approximation,^{2,12}

$$\frac{1}{\zeta_q(t)} = \frac{1}{N\zeta_b} + \frac{1}{3(2\pi)^{3/2} \eta_s N^2} \sum_{n \neq n'} \frac{2 - d_{nn'}^{(q)}}{D_{nn', nn'}^{1/2}(t)}, \quad (12)$$

where η_s denotes the viscosity of the solvent, and ζ_b is the bare friction coming from the diagonal element of the hydrodynamic Oseen tensor.

Finally, let us introduce the formulae for two important observables: the mean squared radius of gyration,

$$R_g^2 = \sum_{q=1}^{N-1} \mathcal{F}_q, \quad (13)$$

and the mean energy,

$$\langle V \rangle = \frac{3}{2} \sum_q k_q \mathcal{F}_q + \sum_{L=2}^{\infty} \hat{u}_L \sum_{m_1 \dots m_L} (\det \Delta^{(L-1)})^{-3/2}. \quad (14)$$

To assist the reader that seeks physical insights into the method we now give a more descriptive version of our approach. Bear in mind that the index q is conjugate to the bead index number n , and therefore \mathbf{x}_q is the amplitude of the internal mode of the chain. Naturally, if there are no intrachain interactions these are normal modes since there

remains only the nearest-neighbor spring term. The basic idea of the Gaussian method is to replace all the intrachain interactions by a matrix of springlike interactions between all pairs of beads on the chain. Then we still have normal modes, but with different spring constants for each mode, these being determined self-consistently from the full interacting potential. At equilibrium the approach is well known and amounts to the claim that we can replace an interacting chain with a “network” of springs with well-chosen spring constants. Accepting the limitations of this method, the current approach extends it to the nonequilibrium situation where all of the spring constants must be chosen in a time-dependent manner to mimic the evolution of the nonequilibrium distribution. This proposition is laid out in Eq. (4). Thus we have different time-dependent spring constants, $\Delta V_q(t)$, for each of the normal modes of the network. Knowing $\Delta V_q(t)$, we can easily calculate all properties of the system including, for example, $\mathcal{F}_q(t)$, which is the ensemble-averaged squared amplitude of the q th Fourier mode at time t . It remains only to determine $\Delta V_q(t)$, and this can be done self-consistently. Thus we apply Eq. (4) and eliminate \mathbf{x}_q everywhere in the exact Langevin equation in favor of ΔV_q . This leads to a self-consistent equation for ΔV_q for time t , given in Eq. (8) and closed via relations (7) and (10). This is basically “the best” time-dependent Gaussian approximation that can be found for a nonequilibrium interacting chain. The whole approach could be extended to non-Gaussian approximants, but common sense indicates that it is wise to start with the simplest approximation. Two final points that may be of interest. First, at equilibrium the method yields the same equations as the Gibbs–Bogoliubov variational approach¹³ based on a Gaussian Hamiltonian that was much used by Feynman.¹⁴ Second, the analytical approach developed here is essentially a time-dependent mean-field theory for the bead and spring model with all the potential problems of such approximation. Our belief that it is useful is based on the fact that it has known equilibrium limits, and the main predictions are in agreement with simulations. In this sense the method of nonequilibrium treatment described above transcends the specific model, and others may wish to pursue it for more detailed polymer models, such as those used in molecular dynamics calculations. That path will require work, but there are no fundamental impediments.

III. NUMERICAL RESULTS

The self-consistency equations (7) and (8) have been studied numerically. Setting the time derivative to zero in Eq. (7) corresponds to the equilibrium situation. Thus, due to Eq. (10), we have a system of $N-1$ nonlinear algebraic equations (8) for determination of the time-independent solution $\Delta V_q^{(e)} = k_B T / \mathcal{F}_q^{(e)}$. This set of equations can be solved iteratively. Note that $q=0$ corresponds to the diffusive mode and does not affect the intramolecular conformational modes. The diffusion constant can be calculated from Eq. (12) as $D = k_B T / \zeta_0$. In the “preaveraging” approximation the hydrodynamic effect does not contribute to the equilibrium effec-

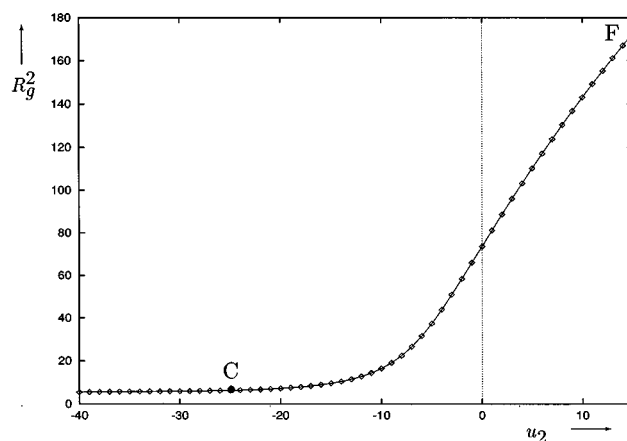


FIG. 1. Plot of the equilibrium mean squared radius of gyration R_g^2 vs the second virial coefficient u_2 for polymer with the degree of polymerization $N=200$ and the third virial coefficient $u_3=10$. In this figure points F and C correspond to the Flory coil and the collapsed globule.

tive potential $\Delta V_q^{(e)}$. It does, however, contribute to the nonequilibrium potential $\Delta V_q(t)$ via Eqs. (12) and (7).

In what follows we shall be interested in kinetics at the collapse transition caused by an abrupt quench to the negative u_2 region. Technically, we start from the equilibrium solution for the Flory coil. Then, after the quench, Eq. (7) is solved using the modified Runge–Kutta scheme.¹⁵ Let us point out that for all the quantities considered in this work the final state of kinetics coincides exactly to that obtained from equilibrium calculations with corresponding parameters.

We restrict ourselves by accounting for the excluded volume effect only up to the three-body interaction, i.e., we set $u_L=0$ for $L>3$. Inclusion of the four-body interaction is important when both u_2 and u_3 are negative. Probably this leads to a set of different collapsed states.¹⁶ However, account of the u_4 term would require quadruple summations¹⁷ in the code, and numerical analysis becomes considerably more time consuming, so we have not attempted to resolve this issue here.

In the sequel we have used the following particular choice of parameters: $k_B T=1$, $\kappa=1$, and $\zeta_b=1$, which provide the units of measurement of temperature, size and time in the system.

A. Equilibrium

We have mentioned in Sec. I, that many aspects of the equilibrium statistical mechanics of polymers are well known.^{1,3,2,18} Therefore, we shall briefly discuss only those results for equilibrium, that demonstrate the advantages and limitations of the Gaussian self-consistent method. This discussion is also necessary as a preliminary for the study of kinetics in Sec. III B.

The typical behavior of the mean squared radius of gyration R_g^2 vs the second virial coefficient u_2 is presented in Fig. 1. The positive and negative u_2 regions correspond to the Flory coil and the collapsed globule respectively. R_g^2

TABLE I. Values of the equilibrium mean squared radius of gyration R_g^2 vs the degree of polymerization N for different values of the second and the third virial coefficients u_2 and u_3 .

N	50	100	150	200	300	400	500
$R_g^2 (u_2=15, u_3=0)$	24.0	62.7	110	163	285	422	572
$R_g^2 (u_2=0, u_3=0.4)$	5.44	11.9	18.9	26.3	42.3	58.9	75.8
$R_g^2 (u_2=-25, u_3=10)$	1.910	3.528	4.956	6.247	8.521	10.50	12.20

scales in the degree of polymerization as $R_g^2 \sim N^{2\nu}$. The values of the swelling exponent, ν , have been calculated from the data of the type presented in Table I,

$$\nu_F = 0.69 \pm 0.01 \quad \text{for good solvent } (u_2=15, u_3=0),$$

$$\nu_\theta = 0.55 \pm 0.02 \quad \text{near the } \theta \text{ point } (u_2=0, u_3=0.4),$$

$$\nu_C = 0.34 \quad \text{for poor solvent}^{19} (u_2=-25, u_3=10).$$

For sufficiently long chains the value of the collapsed exponent tends to $\nu = \nu_C = 1/3$. Nevertheless, the Flory exponent in the Gaussian method tends to the so-called Reiss exponent $\nu = 2/3$, rather than to the correct value $\nu_F = 3/5$, a deficiency of the method that was recognized and understood some time ago.^{2,3,13}

Indeed this limitation was sufficiently serious that a better equilibrium theory was sought by numerous authors. Perhaps the most successful originated in the works of de Gennes ($n \rightarrow 0$ problem¹) for the Flory coil and Lifshitz⁴ for the collapsed state. There was therefore little need to pursue the Gaussian method until one was faced with problems such as kinetics of collapse. Remarkably, as we shall see, the Gaussian method for kinetics gives good agreement with simulation.⁶ It is already known¹¹⁻¹³ that by *ad hoc* application of a cut off the problems at equilibrium are reduced, and one can obtain the normal Flory exponents.

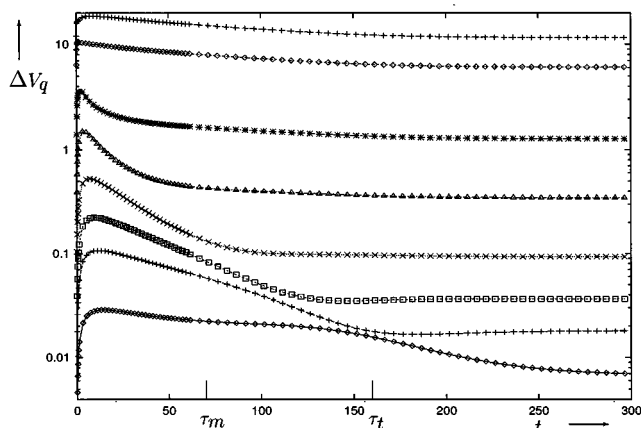


FIG. 2. Plots of the effective potential ΔV_q vs time t for polymer with the degree of polymerization $N=200$ for different values of the chain index q (from bottom to top): $q=1,2,3,5,10,20,50,100$. Initial and final values of the second virial coefficient, the third virial coefficient and viscosity are equal to $u_2=15, u_2'=-25, u_3=10$ and $\eta_s=\infty$ (absence of the hydrodynamic interaction) respectively. Points τ_m and τ_t represent the characteristic time of the second kinetic stage and the "total" collapse time.

The pair correlation functions \mathcal{F}_q and $D_{0n,0n}$ for good solvent scale as,¹¹

$$D_{0n,0n} \sim n^{2\nu}, \quad \mathcal{F}_q \sim q^{-2\beta}, \quad q, n \ll N, \quad \beta = \nu + 1/2. \quad (15)$$

For example, the values of the exponents ν, β found from such scaling laws are $\nu=0.68 \pm 0.01, \beta=1.2 \pm 0.02$ for $N=300$ at point F in Fig. 1. For the collapsed globule (point C in Fig. 1) there is a similar law to Eq. (15) for \mathcal{F}_q with $\beta=0.88 \pm 0.02$. However, $D_{0n,0n}$ increases linearly, then at some cross-over point it saturates to a level that scales as $N^{2/3}$. This is what one would expect from the dense globular state.⁴

The mean energy (14) reaches the asymptotic laws $\langle V \rangle \sim u_2^{2/5}$ for $u_2 \rightarrow \infty$ and $\langle V \rangle \sim -(-u_2/u_3)^2$ for $u_2 \rightarrow -\infty$. The latter theoretical expectations are well justified numerically, but we refrain from presenting the data here because it is rather cumbersome.

B. Kinetics

Now let us consider kinetics after the quench from $u_2 > 0$ to a new value $u_2' < 0$. For an instantaneous quench the effective potential $\Delta V_q(t)$ is discontinuous at the initial time $t=0$ and its jump is proportional to the variation of the second virial coefficient. Nevertheless, $\mathcal{F}_q(t)$ changes continuously since it is related to the effective potential by Eq. (22) of Ref. 12.

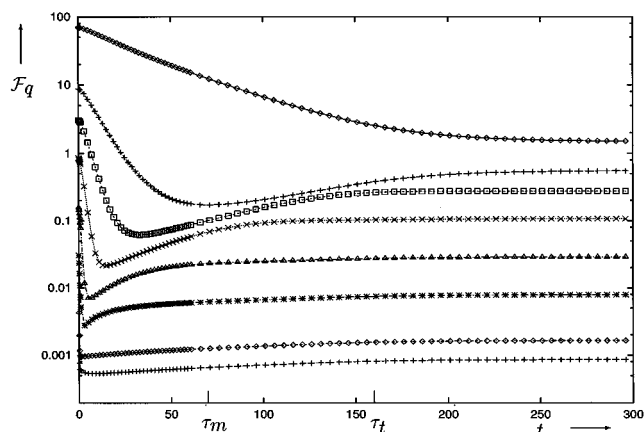


FIG. 3. Plots of the correlation function of the Fourier modes \mathcal{F}_q vs time t for different values of the chain index q (from top to bottom): $q=1,2,3,5,10,20,50,100$. The values of the degree of polymerization, viscosity and virial coefficients are the same as in Fig. 2.

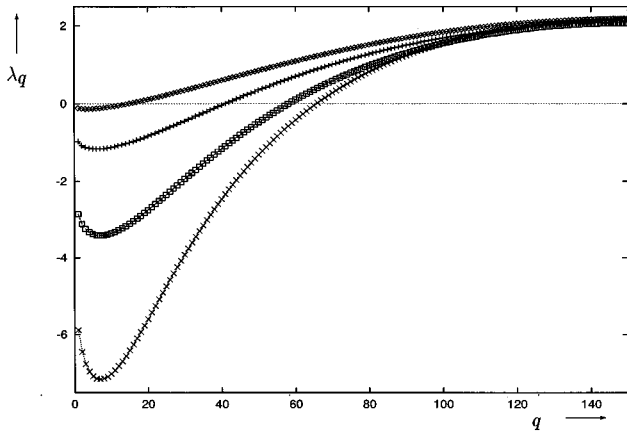


FIG. 4. Plots of the inverse decay rates λ_q vs the chain index q for polymer with the degree of polymerization $N=300$ and viscosity $\eta_s=0.1$. Initial values of the second and the third virial coefficients are equal to $u_2=15$, $u_3=10$ and final values of the second virial coefficient are equal to (from top to bottom): $u'_2 = -5, -25, -50, -70$. Negative values correspond to the region of instability in which modes grow exponentially fast.

In Figs. 2 and 3 we exhibit results of the numerical integration of Eqs. (7) and (8). The behavior of $\mathcal{F}_q(t)$ is natural from the point of view of the “necklace” model of collapse.^{6,7,12} Initially the chain undergoes formation of small locally collapsed globules that grow for some time at the expense of their neighbors in the chain. This process leads to an essential decrease of amplitudes of the large- q modes, these describing the local structure of the chain. There is also a much slower decrease of low- q modes, describing the polymer at large distances along the chain. Let us consider the deviation of \mathcal{F}_q from the initial value for sufficiently small times

$$\Delta \mathcal{F}_q(t) \equiv \mathcal{A}_q (1 - e^{-\lambda_q t}), \quad (16)$$

where we have introduced the Lyapunov exponent λ_q . In Ref. 12 we have analyzed this exponent theoretically using the linearized self-consistency equations and given its interpretation in terms of spinodal decomposition in the internal metric of the chain. Here, it is worthwhile to return to this question and verify our conclusions on the basis of straightforward numerical solution and also to complete the account of the method by incorporating the hydrodynamic interaction.

One may expect certain modifications in the laws due to the fact that the Flory exponent was considered equal to

$\nu_F=3/5$ in Ref. 12 after introduction of a cut off, while indeed it has a larger value here as we have discussed in Sec. III A. We find that this circumstance does not affect the general behavior and conclusions about the existence and properties of unstable modes. In Fig. 4 we draw the Lyapunov exponent λ_q vs the chain index q for different final values of the second virial coefficient. The results are obtained by fitting $\Delta \mathcal{F}_q(t)$ with Eq. (16) for small times. The values of the chain indices of the most unstable mode (i.e., for which $-\lambda_q$ is maximal), q_{\max} , and critical (i.e., the highest unstable) mode, q_c , are presented in Table II. One can see from Table II that they scale with u'_2 in the same way with and without hydrodynamics, although prefactors are somewhat affected by the hydrodynamic interaction. This result may be expected from the linearized approximation, where ζ_q cancels out from the expression for the Lyapunov exponent [Eqs. (35)–(37) in Ref. 12].

The time τ_i , when the critical mode $\mathcal{F}_{q_c}(t)$ reaches its minimum (see Fig. 3), may be considered as the duration of the first kinetic stage. As one can see from Table III, it is fairly independent of the degree of polymerization, thus reflecting the local mechanism of clusters formation at this stage.²⁰

The deviation of the mean squared radius of gyration at this spinodal stage may be estimated for small quenches when the contribution of unstable modes is negligible. Using Eq. (16) we write

$$\Delta R_g^2(t) = \sum_{q>q_c} \frac{B_q}{\zeta_q \lambda_q} (1 - e^{-\lambda_q t}), \quad (17)$$

where the parameters are estimated using formulas (35), (38), and (39) of Ref. 12

$$B_q \sim \mathbf{q}^{3\nu-2}, \quad \lambda_q \sim \mathbf{q}^{2\nu+1}, \quad (18)$$

with $\mathbf{q}=2\pi q/N$. According to Ref. 11 the friction scales as $\zeta_q \sim \mathbf{q}^{1-\nu}$ with hydrodynamics and it is a constant in the absence of hydrodynamics. Converting the sum into integral we obtain the law for small quenches,

$$\Delta R_g^2(t) = -A t^{\alpha_i}, \quad t < 1/|\lambda_{q_{\max}}|, \quad (19)$$

$$\alpha_i = \begin{cases} \frac{3-2\nu_F}{2\nu_F+1} & \text{with hydrodynamics,} \\ \frac{2-\nu_F}{2\nu_F+1} & \text{without hydrodynamics,} \end{cases}$$

TABLE II. Values of the chain indices of the critical, q_c , and maximal, q_{\max} , unstable modes vs the final value of the second virial coefficient, u'_2 , for polymer with the degree of polymerization $N=300$ and $u_2=15$, $u_3=10$. Here, the quantity δ denotes the exponent of appropriate chain index in $|u'_2|$, i.e., $q \sim |u'_2|^\delta$.

u'_2	-5	-10	-15	-25	-35	-50	-70	δ
q_c ($\eta_s=\infty$)	16	25	32	43	51	61	70	0.56 ± 0.04
q_c ($\eta_s=0.1$)	15	24	31	41	49	58	67	0.56 ± 0.05
q_{\max} ($\eta_s=\infty$)	4	6	7	8	9	10	11	0.37 ± 0.06
q_{\max} ($\eta_s=0.1$)	3	4	5	6	7	7	8	0.37 ± 0.06

TABLE III. Values of the characteristic collapse times τ_i , τ_m , τ_r , and τ_f vs the degree of polymerization N for different viscosities η_s . In this table $u_2=15$, $u_2' = -25$ and $u_3=10$. Here, the quantity γ denotes the exponent of the appropriate time in terms of the degree of polymerization, i.e., $\tau \sim N^\gamma$. Note that the limit $\eta_s = \infty$ corresponds to absence of hydrodynamics, whilst $\eta_s=0.1$ describes the regime of strong hydrodynamic effect, and $\eta_s=0.5$ corresponds to the crossover region (see also the caption to Fig. 6).

N	30	50	70	100	150	200	300	γ
$\tau_i (\eta_s = \infty)$	1.25	1.47	1.56	1.59	1.61	1.63	1.64	0.05 ± 0.03
$\tau_i (\eta_s = 0.5)$	1.12	1.23	1.36	1.38	1.41	1.44	1.47	0.08 ± 0.04
$\tau_i (\eta_s = 0.1)$	0.72	0.90	0.99	1.08	1.13	1.15	1.18	0.10 ± 0.06
$\tau_m (\eta_s = \infty)$	1.8	4.4	8.3	16.6	38	70	156	2.00 ± 0.03
$\tau_m (\eta_s = 0.5)$	1.4	3.2	5.6	10.2	20.7	34.5	71.7	1.71 ± 0.03
$\tau_m (\eta_s = 0.1)$	0.93	1.4	2.6	4.2	7.5	11.8	22.3	1.48 ± 0.04
$\tau_r (\eta_s = \infty)$	3.9	10.5	20.3	40.8	90.7	160.3	357	1.96 ± 0.01
$\tau_r (\eta_s = 0.5)$	3.0	7.1	12.0	22.0	42.6	67.6	129	1.63 ± 0.02
$\tau_r (\eta_s = 0.1)$	1.7	3.2	5.0	8.1	14.0	21.0	37.3	1.34 ± 0.03
$\tau_f (\eta_s = \infty)$	1.18	2.97	5.49	10.2	20.6	33.0	65.7	1.74 ± 0.03
$\tau_f (\eta_s = 0.5)$	0.975	2.02	3.16	4.96	8.83	13.2	23.4	1.37 ± 0.02
$\tau_f (\eta_s = 0.1)$	0.612	1.10	1.58	2.19	3.41	4.47	7.02	1.04 ± 0.03

where ν_F is the Flory exponent. Numerically for $u_2' = -5$ we have obtained the values of the exponent $\alpha_i = 0.83 \pm 0.02$ ($\alpha_i = 0.66 \pm 0.02$) with (without) hydrodynamics. These numbers are fairly close to the expected theoretical predictions.²¹ It is important to emphasize that deeper quenches give rise to an essential contribution of unstable modes and the law (19) is violated leading to a higher exponent α_i .

The second, or coarsening stage, takes much longer than the spinodal process. During this stage unstable modes change their decrease to a slow increase (see Fig. 3). The increase describes the process of mixing of the original small clusters within larger ones after unification. We note that the first mode describes the conformation of the polymer as the whole and it is always a monotonically decreasing function of time. It is also interesting to consider the time τ_m , when the second internal mode \mathcal{F}_2 has its minimum amplitude. The quantity τ_m may be considered as a characteristic time of the second kinetic stage. In Table III we present values of τ_m for different degrees of polymerization and viscosities. The characteristic time scales with the degree of polymerization according to $\tau_m \sim N^{\gamma_m}$, where $\gamma_m = 3/2$ ($\gamma_m = 2$) with (without) hydrodynamics (see Table III). In other words, τ_m scales as the Zimm (Rouse) relaxation time. In this sense, one can say that the coarsening stage of collapse is dominated by the behavior of the ideal Gaussian coil. This is in agreement with the phenomenological theory of de Gennes,⁹ and with Monte Carlo calculations.⁶

In Fig. 5 we exhibit the evolution of the mean squared radius of gyration in kinetics for different viscosities of solvent. One can see that the hydrodynamic effect leads to a more rapid collapse, especially at the coarsening stage. This has a simple explanation. Indeed, the diffusion constant of a locally collapsed cluster consisting of M monomer units scales as $D \sim M^{-1}$ if we neglect hydrodynamics, but as $D \sim M^{-1/3}$ when the hydrodynamic effect dominates. Thus with hydrodynamics these clusters possess a higher mobility, and the total mobility of the polymer is growing during kinetics. The diffusion constant of the whole chain, $D(t) = k_B T / \zeta_0(t)$, and the inverse friction of the first mode

are presented in Fig. 6 as functions of time. The former is monotonically increasing, and the latter behaves initially in the same manner until the internal friction within the collapsing globule leads to decrease and saturation.

The final stage of collapse is a slow process of shape optimization and compaction of the globule. It is described by a single exponential relaxation of the internal modes and effective potential towards the final equilibrium state. Clearly it is, strictly speaking, impossible to distinguish precisely between the second and the final stages. Let us introduce what we call the “total” collapse time, τ_t , as that time, when a single exponential approximation begins to work reliably well for the radius of gyration. For example, for the chain lengths we have considered, this may be chosen as that time, when the squared radius of gyration has passed through 99% of its overall change: $R_g^2(\tau_t) = 0.01R_g^2(0) + 0.99R_g^2(\infty)$. In Table III we show the final relaxation time τ_f determined

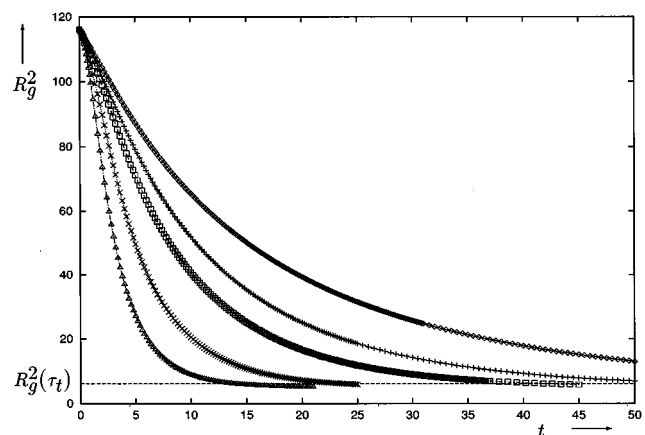


FIG. 5. Plots of the square radius of gyration $R_g^2(t)$ vs time t for polymer with the degree of polymerization $N=150$ for different viscosities η_s (from bottom to top): 0.1, 0.2, 0.5, 1.0, ∞ . The values of the virial coefficients are equal to $u_2=15$, $u_2' = -25$, $u_3=10$. The dash line denotes the value of the squared radius of gyration at the moment equal to the total collapse time.

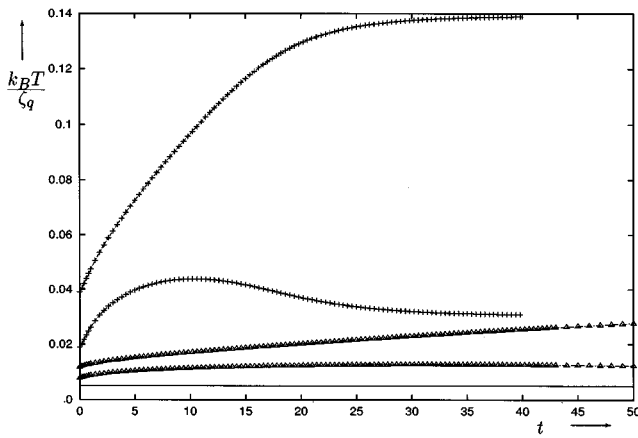


FIG. 6. Plots of the inverse friction coefficients $k_B T / \zeta_q(t)$ vs time t for polymer with the degree of polymerization $N=200$. The curves correspond to (from top to bottom): $q=0$ (the diffusion coefficient) and $q=1$ at the viscosity $\eta_s=0.1$, $q=0$ and $q=1$ at the viscosity $\eta_s=0.5$. The value $\eta_s=0.1$ corresponds to the regime of strong hydrodynamic effect, for which contribution of the bare mobility term is negligible in ζ_q for small q . The values of the virial coefficients are equal to $u_2=15$, $u_2'=-25$, $u_3=10$. The straight solid line denotes the value of the inverse friction coefficients without hydrodynamics ($\eta_s=\infty$).

from the mean squared radius of gyration $R_g^2(t) = R_g^2(\infty) + A_f e^{-t/\tau_f}$, or equivalently the time-scale deduced from the first internal mode $\mathcal{F}_1(t)$. Thus we find $\tau_f \sim N^{\gamma_f}$, where $\gamma_f=1$ ($\gamma_f=5/3$) with (without) hydrodynamics.²² Therefore, it is proportional to the equilibrium relaxation time of the final collapsed state $\tau_c \sim N^{3\nu_c}$ ($\tau_c \sim N^{2\nu_c+1}$) with (without) hydrodynamics, where $\nu_c=1/3$ is the collapsed swelling exponent. Naturally, the “total” collapse time should obey $\tau_t > \tau_m$, and scaling of the exponent γ_t , where $\tau_t \sim N^{\gamma_t}$, is some cross-over between the exponents γ_m and γ_f (see Table III) with $\gamma_t \rightarrow \gamma_m$ when $N \rightarrow \infty$. Thus for sufficiently long chains, the main collapse takes a finite time about $\tau_t \sim N^{\gamma_m}$,²³ and then the process is exponentially slow with the time characterized by universal exponent γ_f .

Finally, we would like to discuss the kinetic laws as a function of the depth of the quench, by which we mean the deviation from the θ -point, $|u_2'|$, and the third virial coefficient, u_3 . Our analysis has led us to conclude that the characteristic collapse times depend on N , $|u_2'|$ and u_3 as power laws independently in each parameter over a wide range of numerical values. The scaling exponents of the times τ_m and

τ_f in terms of the depth of the quench are close to the law $\tau_{m,f} \sim |u_2'|^{-2}$ (see Table IV) for deep quenches, irrespective of the hydrodynamic interaction. Thus the deeper the quench, the more rapid is collapse due to stronger two-body attraction. Similarly, from the results of Table V scaling exponents are obtained in terms of the third virial coefficient: $\tau_m \sim u_3$, $\tau_f \sim u_3^{3/2}$. Qualitatively then, higher third virial coefficient gives rise to stronger three-body repulsion and slows collapse rate.

IV. CONCLUSION

In this paper we have studied the kinetic laws of the collapse transition of a homopolymer by numerical solution of the equations obtained in the Gaussian self-consistent approach. Although the conformations of an individual polymer during kinetics are complex, as is the evolution of the internal modes, it is remarkable that the analysis leads to a number of very simple universal laws corresponding to different kinetic stages. We can see three stages of the process: a rapid spinodal process is characterized by the set of Lyapunov exponents λ_q and the law $R_g^2(t) = R_g^2(0) - At^{\alpha_i}$ for small quenches with α_i given by Eq. (19); the coarsening stage is dominated by the ideal Gaussian coil ($\nu_\theta=1/2$) behavior with its characteristic time $\tau_m \sim N^{3\nu_\theta} |u_2'|^{-2} u_3$; a slow relaxational stage towards the final equilibrium globule ($\nu_c=1/3$) which is exponentially slow with a time $\tau_f \sim N^{3\nu_c} |u_2'|^{-2} u_3^{3/2}$. We have also studied dependence on the viscosity of the solvent.

A strong argument in favour of our results is the good agreement with Monte Carlo simulation performed without hydrodynamics.⁶ Namely, we find the same qualitative picture in the behavior of the internal modes and good agreement in the values of the kinetic exponents α_i and γ_m . The exponent γ_f has not been studied in Ref. 6 due to computational difficulties. Given the significant difference between approaches and acknowledging that each has their own disadvantages and limitations, such agreement encourages us to believe that we are really seeing the correct universal properties for homopolymer kinetics within the current model. In addition, visualization of polymer conformations in the Monte Carlo simulation provides us with a simple physical interpretation and understanding of the kinetic laws in terms of cluster formation and growth.⁶ Namely, the spinodal stage corresponds to the formation of small locally collapsed clusters along the chain or a “necklace” of clusters; the coarsen-

TABLE IV. Values of the characteristic collapse times τ_m , τ_t , and τ_f vs the final value of the second virial coefficient u_2' for different viscosities η_s . In this table $N=150$, $u_2=15$ and $u_3=10$. Here, the quantity δ_2 denotes the exponent of the appropriate time in terms of the final second virial coefficient $|u_2'|$, i.e., $\tau \sim |u_2'|^{\delta_2}$.

u_2'	-5	-10	-15	-25	-35	-50	-70	δ_2
τ_m ($\eta_s=\infty$)	294	173	97	38	19.4	9.55	4.74	-1.96 ± 0.05
τ_m ($\eta_s=0.1$)	80	41.2	21.2	7.5	3.65	1.70	0.92	-2.05 ± 0.05
τ_t ($\eta_s=\infty$)	1071	482	240	90.7	43.5	19.0	7.84	-2.2 ± 0.1
τ_t ($\eta_s=0.1$)	233	93.5	42.1	14.0	6.75	2.65	1.33	-2.27 ± 0.08
τ_f ($\eta_s=\infty$)	271	109	50.0	20.6	10.5	4.58	2.21	-2.0 ± 0.1
τ_f ($\eta_s=0.1$)	63.1	24.7	10.4	3.41	1.78	0.69	0.32	-2.2 ± 0.1

ing stage describes their unification with the law of cluster population growth $s \sim t^{1/\gamma_m}$, which is a generalization of the Lifshitz–Slyozov law; shape optimization and compaction of the globule is the final exponential stage.

An important deficiency of the Gaussian method is that it yields an incorrect Flory exponent. The reason is well understood and the problem may be addressed in different ways.^{11,13} One has to be sure that this drawback of the Gaussian theory does not affect the kinetic laws. The problem is inherent only in the Flory coil state, and it would be reasonable to expect that it would modify only the early stages of kinetics. This conjecture is indeed justified by comparison to the Monte Carlo simulation. Thus instead of naively interpreting the numerical values of the exponent α_i , we have derived formula (19) with the Flory exponent as a free parameter. Substitution of the correct value of ν_F leads to a value α_i , that turns out to be quite close to the value of Ref. 6.

Another deficiency of the method is that the chain is fundamentally phantom, that is it can pass through itself. This may become an essential limitation in the dense globular state. Due to topological restrictions the late state of kinetics for a nonphantom chain will have a different structure than for a phantom one. For an open polymer topological restrictions may be removed via self-reptations of the chain, and it has been argued that this leads to an even longer final kinetic stage with the time scale¹⁰ $\tau_{\text{reptations}} \sim N^3$. This is a really delicate question and it is not quite settled at the moment. One may suggest a special Monte Carlo technique²⁴ as a possible way to proceed in that direction. Practically speaking, the issue of topology does not modify the kinetic stages and laws we have considered, but could only add the fourth very long-lived relaxational stage.

Having reached a degree of comfort with the method, we now turn to the validity of the model itself. This Edwards-style model is well validated for equilibrium calculations, but not for kinetics. It is an inherently coarse-grained model where the low-energy conformational barriers have been integrated out. At equilibrium there is little doubt that this is acceptable. As for a dynamical model, we must be assured that whatever local backbone conformational barriers are to be overcome for the initial stage of clustering to take place, they are small enough to represent shorter time scales than those we study. Whether this is indeed true probably depends

on the polymer, solvent and temperature jump, but we cannot, within the current treatment, address such issues. There are early indications from both experiment²⁵ and molecular dynamics⁸ that such issues may be important.

In summation then, we have presented a general approach to the study of nonequilibrium phenomena where the fractal dimension may change, and applied it rather fully to the homopolymer collapse problem. We believe that the essential features of kinetic laws of the Edwards-type model are now resolved, and that the method we describe is useful and will increasingly prove its worth in problems such as the kinetics of periodic and random copolymers,²⁶ protein and DNA folding. It seems likely that the method gives for many such problems good qualitative and in some cases quantitative predictions. One should note that this assessment is based on our experience with a particular class of problems and the intuitions based on these so, in time, later applications may lead to some revision of these positive views.

If we accept this estimate of the current situation then what can one hope to achieve in the biopolymer and heteropolymer field? Evidently, as with homopolymer, if there are new universal kinetic laws for these systems they are not readily derived, and have not yet been given in the literature. Natural extensions of the method we have discussed will permit one to deduce both the folding mechanism and the laws. Our preliminary conclusion from this approach is that various mechanistic ideas already in the literature will be strengthened and quantitative laws added to them. Apart from the attraction of such information to the physical scientist, there may be practical implications also in terms of identifying chemical sequence structure to time-scale relations. In turn this may lead to novel algorithms to explore more complex biopolymer calculations where a realistic chemical structure would be the product. Such considerations, in our opinion, justify the current high level of effort directed at heteropolymers by numerous researchers. These issues, along with the fact that complete understanding of the homopolymer kinetic problem will continue to be the entry price to progress in quantitative biopolymer studies, justify a continuing interest in the homopolymer case beyond what we have presented. We believe this work could be progressed in the direction of less coarse-grained homopolymer models than we have studied, thereby finally securing one more pe-

TABLE V. Values of the initial and final radii of gyration and of the characteristic collapse times τ_m , τ_i , τ_f vs the third virial coefficient u_3 without hydrodynamics ($\eta_s = \infty$). In this table $N=150$, $u_2=15$ and $u_2' = -25$. Here, the quantity δ_3 denotes the exponent of the appropriate time scale in terms of the third virial coefficient u_3 , i.e., $\tau \sim u_3^{\delta_3}$, where δ_3 is found to be the same with and without hydrodynamics. Note that the squared radius of gyration is almost independent of u_3 for the Flory coil, whilst it scales as $R_g^2 \sim u_3^{2/3}$ for the collapsed globule in agreement with Ref. 11.

u_3	1	2	5	10	15	20	δ_3
$R_g^2(0)$	110.5	111.1	113.0	116.0	118.7	121.3	0.03 ± 0.01
$R_g^2(\infty)$	1.40	2.10	3.32	4.96	7.14	9.63	0.63 ± 0.07
τ_m	3.57	6.40	17.3	38.0	62	85	1.07 ± 0.05
τ_i	4.55	9.62	35.5	90.7	154	227	1.33 ± 0.05
τ_f	0.745	2.07	8.05	20.6	34.7	53.8	1.42 ± 0.03

rimeter in the scientific attack on the heteropolymer and biopolymer problem.

Finally we would also comment that there are other possible applications of our method. For example, the kinetics of gels, networks or fragile glasses may offer opportunities for future applications. In addition, the type of example we study could equally well have emerged from a quantum path-integral calculation for an isolated electron in a solvent that induces a trajectory with certain effective interactions. In the case of electron localization the wave function may be conceived instead in terms of a path-integral, and then the basic machinery that we describe here can be used to study the kinetics of localization or electron transfer after a rapid change in the environment. Such issues will be discussed by us elsewhere, but possibly others with a tradition in these fields will find this an interesting pursuit.

ACKNOWLEDGMENTS

The authors acknowledge interesting discussions with Professor B. Chu, Professor P. G. de Gennes, Professor A. Yu. Grosberg, Professor A. R. Khokhlov, Professor P. Pincus, Professor Y. Rabin and Dr. A. Gorelov who have offered various insights into collapse kinetics. We are also grateful to our colleague P. Kiernan for assistance. This work was supported by DEC and the Irish Government.

APPENDIX: RING VS OPEN POLYMERS IN THE GAUSSIAN SELF-CONSISTENT METHOD

In this Appendix we generalize our treatment of Sec. II to include both ring and open polymers. Thus let us consider in parallel two homopolymers, one of which is a ring constituted of N_r beads and another one is open with N_o beads. For a ring polymer one has cyclic boundary condition $\mathbf{x}_{n+N_r} = \mathbf{x}_n$ for all n , while there is no special restriction on the conformations of open polymer. However, to treat the open polymer it is useful to formally introduce the fictitious beads with the chain indices $n = -1$ and $n = N_o$, such that their positions satisfy the discreet Neumann boundary condition $\mathbf{x}_{-1} = \mathbf{x}_0$ and $\mathbf{x}_{N_o} = \mathbf{x}_{N_o-1}$.

We begin with a mathematical question about the proper definition of the independent modes. Let us introduce the following notations:

Ring	Open
$f_n^{(q)} = \exp(i2\pi qn/N_r)$,	$f_n^{(q)} = \cos(\pi q(n+1/2)/N_o)$,
$\epsilon^{(q)} = -4 \sin^2(\pi q/N_r)$,	$\epsilon^{(q)} = -4 \sin^2(\pi q/2N_o)$,
$\gamma_q = 1$,	$\gamma_q = 2 - \delta_{q0}$.

(A1)

Then the Fourier transform may be defined in the general form

$$\mathbf{x}_q = \frac{\gamma_q}{N} \sum_{n=0}^{N-1} f_n^{(q)} \mathbf{x}_n, \quad \mathbf{x}_n = \sum_{q=0}^{N-1} f_n^{(-q)} \mathbf{x}_q, \quad (A2)$$

where $N = N_r, N_o$ for ring and open polymer respectively. Indeed, $f_n^{(q)}$ may be treated as eigenfunctions and as $\epsilon^{(q)}$ eigenvalues of the discreet second derivative operator Δ ,

$$\Delta f_n^{(q)} \equiv f_{n+1}^{(q)} + f_{n-1}^{(q)} - 2f_n^{(q)} = \epsilon^{(q)} f_n^{(q)} \quad (A3)$$

with corresponding boundary conditions. Thus the set $\{\sqrt{\gamma_q/N} f_n^{(q)}\}$ is a complete and orthonormal basis. For ring polymers this basis is well known, whilst for open polymers its properties can be easily established using the relation connecting it with the Chebyshev polynomials

$$f_n^{(q)} = U_n(f_1^{(q)}) - U_{n-1}(f_1^{(q)}), \quad (A4)$$

$$U_n(x) = (1-x^2)^{-1/2} \sin((n+1)\arccos x). \quad (A5)$$

There is a fundamental distinction between ring and open polymers due to topology. This, however, is irrelevant as long as we consider only phantom chains. The Gaussian self-consistent method may be developed for open polymers in quite a similar manner to rings. The important point is that, strictly speaking, the effective potential should be non-diagonal $\Delta V_{qq'}$ there, whilst its diagonal property is exact for rings. It is well established that, at equilibrium, the values of the universal exponents are different in the middle of the chain and near the ends.³ The difference however is rather small and could not be deduced at the mean-field level, which our approach actually represents. We have explicitly checked in simulations that no end-effects dominate kinetics. Thus in our method it is sufficient to keep only the diagonal elements of the effective potential for sufficiently long chains. Physically, this is equivalent to the property that the spatial correlations $\langle (\mathbf{x}_m - \mathbf{x}_m')^2 \rangle$ depend only on the difference $|m - m'|$. It is known that this is valid for finite chains when $|m - m'|$ is sufficiently large. In other words, neglect of the nondiagonal elements affects only properties of the chain at short distances and does not change any of its global characteristics such as the radius of gyration. The bigger the chain length the better the precision of the diagonal method.

Bearing in mind these reservations, the self-consistency equation (7) remains valid for both cases. The effective potential may be written in terms of the mean energy (14) as follows:

$$\Delta V_q = \frac{2}{3} \frac{\partial \langle V \rangle}{\partial \mathcal{F}_q}. \quad (A6)$$

Formula (9) for the matrix $\Delta^{(L-1)}$ is also valid. However, formulas for the friction, ζ_q , connectivity coefficients, k_q , and connection (10) between the spatial correlations and the Fourier modes should be generalized,

$$\zeta_q = \frac{N}{\gamma_q} \zeta_b, \quad k_q = \frac{N}{\gamma_q} \kappa |\epsilon^{(q)}|, \quad (A7)$$

$$D_{nn',nn'} = \sum_{q=1}^{N-1} d_{nn'}^{(q)} \mathcal{F}_q, \quad d_{nn'}^{(q)} = |f_n^{(q)} - f_{n'}^{(q)}|^2. \quad (A8)$$

Similarly, the squared radius of gyration is given by,

$$R_g^2 = \frac{1}{\gamma_1} \sum_{q=1}^{N-1} \mathcal{F}_q. \quad (A9)$$

The crucial observation is that the spatial correlations for open polymer may be decomposed,

$$D_{mm',mm'} = \frac{1}{2} D_{|m-m'|} + \frac{1}{2} C_{mm'}, \quad (\text{A10})$$

$$D_{|m-m'|} = 4 \sum_{q=1}^{N_o-1} \sin^2 \frac{2\pi q(m-m')}{N_o} \mathcal{F}_q, \quad (\text{A11})$$

$$C_{mm'} = \sum_{q=1}^{N_o-1} \left(2 \cos \frac{2\pi q(m+m'+1)}{N_o} - \cos \frac{2\pi q(2m+1)}{N_o} - \cos \frac{2\pi q(2m'+1)}{N_o} \right) \mathcal{F}_q. \quad (\text{A12})$$

The first term $D_{|m-m'|}$ is analogous to the expression for the spatial correlation of ring polymer. The sum in the second term is rapidly oscillating and for large N_o is negligible. Hence at the level of our mean-field approximation open and ring chains become equivalent for sufficiently large degrees of polymerization.

Note that for ring polymers only half of the Fourier modes are independent due to the relation $\mathcal{F}_{N_r-q} = \mathcal{F}_q$. This, together with explicit formulas (A1), allows one to establish a connection between ring and open polymers for large degrees of polymerization satisfying condition $N_r = 2N_o$. Given that their connectivity constants and virial coefficients are in the relations,

$$\kappa^{\text{ring}} = \kappa^{\text{open}}, \quad u_L^{\text{ring}} = 2^{1-L} u_L^{\text{open}}, \quad (\text{A13})$$

the radii of gyration and spatial correlations of both chains will be equal. This statement is valid at equilibrium as well as for kinetics. It generalizes the well known observation that ideal ring chains are more compact than open ones with the equal number of units,⁴ $R_g^{\text{ring}} = R_g^{\text{open}}/\sqrt{2}$. As we have seen it is more natural to compare ring chains with twice as many units as open ones and appropriately redefined virial coefficients (A13).

¹P. G. de Gennes, *Scaling Concepts in Polymer Physics* (Cornell University, Ithaca, 1988).

²M. Doi and S. F. Edwards, *The Theory of Polymer Dynamics* (Oxford Science, New York, 1989).

³J. des Cloizeaux and G. Jannink, *Polymers in Solution* (Clarendon, Oxford, 1990).

⁴A. Yu. Grosberg and A. R. Khokhlov, *Statistical Physics of Macromolecules* (AIP, New York, 1994).

⁵B. Ostrovsky and Y. Bar-Yam, *Comput. Polym. Sci.* **3**, 9 (1993); M. A. Smith, Y. Bar-Yam, Y. Rabin, B. Ostrovski, C. A. Bennett, N. Margolus, and T. Toffoli, *Comput. Polymer Sci.* **2**, 165 (1992).

⁶Yu. A. Kuznetsov, E. G. Timoshenko, and K. A. Dawson, *J. Chem. Phys.* **103**, No 11, 4807 (1995).

⁷A. Byrne, P. Kiernan, D. Green, and K. A. Dawson, *J. Chem. Phys.* **102**, 573 (1995).

⁸T. A. Kavassalis and P. R. Sundrarajan, *Macromolecules* **26**, 4144 (1993); G. Tanaka and W. L. Mattice, *ibid.* **28**, 1049 (1995).

⁹P. G. de Gennes, *J. Phys. Lett.* **46**, L639 (1985).

¹⁰A. Yu. Grosberg and D. V. Kuznetsov, *Macromolecules* **26**, 4249 (1993).

¹¹E. G. Timoshenko and K. A. Dawson, *Phys. Rev. E* **51**, No 1, 492 (1995).

¹²E. G. Timoshenko, Yu. A. Kuznetsov, and K. A. Dawson, *J. Chem. Phys.* **102**, No 4, 1816 (1995).

¹³D. Bratko and K. A. Dawson, *J. Chem. Phys.* **99**, 5352 (1993).

¹⁴R. Feynman, *Statistical Mechanics* (Benjamin, Reading, 1972).

¹⁵*Numerical Recipes in C*, edited by W. H. Press, S. A. Teukolsky, W. T. Vetterling, and B. P. Flannery (Cambridge University, Cambridge, 1992).

¹⁶Yu. A. Kuznetsov, E. G. Timoshenko, and K. A. Dawson, *J. Chem. Phys.* **104**, 336 (1996).

¹⁷In fact, due to cyclicity one of summations over $m_1 \cdots m_L$ in Eq. (8) can be reduced. However, there are $N-1$ equations to solve, so the total number of summations necessary to perform an iteration grows as N^L in the problem with u_L term.

¹⁸G. Allegra and F. Ganazzoli, *J. Chem. Phys.* **83**, 397 (1985).

¹⁹This number for the collapsed exponent has been obtained by an extrapolation of ν using the data for $N=400, 500$ from Table I, rather than by a direct fitting procedure, which would give a worse agreement for short polymer chains.

²⁰Such a definition is well defined for deep and moderate quenches when the number of unstable modes is not too small.

²¹The result (19) for α_i is valid irrespective of the value of the Flory exponent ν_F . It means that in the improved theory (Ref. 13) one would have $\nu_F=3/5$ and $\alpha_i=9/11(7/11)$ with (without) hydrodynamics.

²²Strictly speaking, from the data of Table III we only get that $\gamma_f=3\nu_c(\gamma_f=2\nu_c+1)$ with (without) hydrodynamics, where ν_c is the measured value of the collapsed exponent [see discussion after Eq. (15) and Ref. 19]. But for $N \rightarrow \infty$ we have $\nu_c \rightarrow 1/3$ and $\gamma_f \rightarrow 1(5/3)$.

²³Our fitting suggests that one can define $\tau_i = a\tau_m + b\tau_f$, where $a > 1$ and b are fixed N -independent factors, so that starting from τ_i a single exponential approximation works well. Then for $N \rightarrow \infty$ we shall have $\tau_i \sim \tau_m$.

²⁴A. Yu. Grosberg, Yu. A. Kuznetsov, E. G. Timoshenko, and K. A. Dawson (unpublished, 1995).

²⁵B. Chu (unpublished); A. Gorelov, K. A. Dawson, *Macromolecules* (submitted).

²⁶E. G. Timoshenko, Yu. A. Kuznetsov, and K. A. Dawson, *Phys. Rev. E* (in press).